This is a repository copy of *Adjoint error estimation and spatial adaptivity for EHL-like models*.

Published paper

AJOINT ERROR ESTIMATION AND SPATIAL ADAPTIVITY FOR EHL-LIKE MODELS
Error Estimation for EHL

Dan Hart[1], Christopher E Goodyer[1], Martin Berzins[1,2], Peter K Jimack[1], and Laurence Scales[1,3]

[1] *University of Leeds, Leeds, LS2 9JT, UK;* [2]*SCI Institute, University of Utah, Salt Lake City, Utah, USA;* [3]*Shell Global Solutions, Cheshire Innovation Park, Chester, UK*

Abstract: The use of adjoint error estimation techniques is described for a model problem that is a simplified version of an EHL line contact. Quantities of interest, such as friction, may be dependent upon the accuracy of the solution in some parts of the domain more than in others. The use of an inexpensive extra solve to calculate an adjoint solution is described for estimating the inter-grid error in the value of friction calculated, and as a basis for local refinement. It is demonstrated that this enables an accurate estimate for the quantity of interest to be obtained from a less accurate solution of the model problem.

Key words: Error estimation, discrete adjoint, EHL, friction calculation, mesh adaptation

1.   INTRODUCTION

Numerical simulations of lubrication problems are of great benefit to industry for the design and evaluation of both oils and contacts since laboratory experiments are costly in terms of both time and money. Simulations enable a much wider range of cases to be evaluated provided that appropriate physical and mathematical models are used, and that the software is fast, robust and accurate.

One potential vehicle for allowing these requirements to be met is the use of *a posteriori* error estimation combined with spatial mesh adaptation, where more points are placed in regions where the solution is sensitive to the local resolution and fewer points where it is insensitive. These ideas are not new to computational engineering and have been used in problems such as

elastohydrodynamic lubrication (EHL) by a number of authors[1,2,3,4,5,6].   In this paper we note that, when solving such problems, the goal of the engineer may typically be to obtain knowledge about some quantity that may be derived from the solution, such as the total friction through the contact for example. For this reason it may not always be most efficient to develop the mesh adaptation strategy so as to maximise the overall increase in the accuracy of the computed solution, since this may have relatively little effect on the quantity of interest.

In this work we consider an alternative mechanism for controlling mesh adaptivity for EHL-like problems, based upon controlling the error in the quantity of interest, the calculated friction for example, rather than the solution as a whole. This is achieved at the relatively small expense of solving an additional problem which yields an approximation to an adjoint solution. Using an adjoint system to gain extra information about a solution has long been exploited in optimal shape design[7], and recently these ideas have become common in aerospace engineering[8,9].

In the case of EHL an additional complicating factor is the presence of cavitation which leads to a free boundary in the mathematical model. An initial investigation into the application of adjoints to this type of problem has been made by Hart *et al*[10], where the free boundary problem was considered in the context of uniform mesh refinement only. In this work we extend the approach to demonstrate that the adjoint solution can also yield local information that may be used to drive non-uniform refinement in an effective manner. Furthermore it is shown how varying the quantity of interest results in different local refinement patterns.

The following section provides an outline of the theory that lies behind adjoint error estimation whilst Section 3 describes the nonlinear, free-boundary, model problem being solved. Results are then shown in Section 4 illustrating the accuracy of the error estimator that has been implemented, as well as the performance of mesh adaptation based upon this. The paper concludes with a short discussion of the material presented and of the directions in which ongoing research is headed.

2.   ADJOINT ERROR ESTIMATION THEORY

In this section, the abstract background to the adjoint estimation of an error is introduced. The starting point is to define two meshes with spacing $h = \Delta x$ and $H = \Delta X = m \times \Delta x$ (m some integer > 1). The idea is that mesh size H is fine enough to capture the features of the problem being solved, and coarse enough to be solved in a reasonable time, while the fine

mesh size h would give the solution to a greater accuracy but in an unacceptable time.

Consider an arbitrary problem whose discrete form may be represented as $A_h u_h = f_h$ on the finer mesh, and $A_H u_H = f_H$ on the coarser mesh. Let u_h^H be an approximation to u_h obtained by interpolation of the coarse mesh solution: $u_h = I_h^H u_H$. A Taylor series expansion for the fine grid residual function $R_h(u_h) = f_h - A_h u_h$ as explained by Darmofal and Venditti[9], shows that

$$
\begin{aligned}
0 = R_h(u_h) &= R_h(u_h^H + (u_h - u_h^H)) \\
&= (f_h - A_h u_h^H) + \left[\frac{\partial R_h}{\partial u_h} \bigg|_{u_h^H} \right](u_h - u_h^H) + h.o.t.
\end{aligned} \tag{1}
$$

Neglecting higher order terms, (1) may be written as

$$
(u_h - u_h^H) = -\left[\frac{\partial R_h}{\partial u_h} \bigg|_{u_h^H} \right]^{-1} (f_h - A_h u_h) \tag{2}
$$

Suppose that the quantity of interest for this problem is a functional which may be expressed as $F_h(u_h)$ on the finer grid. This can also be expanded about the interpolated coarse mesh solution to give

$$
F_h(u_h) = F_h(u_h^H) + \left(\frac{\partial F_h}{\partial u_h} \bigg|_{u_h^H} \right)^T (u_h - u_h^H) + h.o.t.
$$

Expression (2) may be substituted into this and, again discounting higher order terms, this becomes

$$
F_h(u_h) = F_h(u_h^H) - \left(\frac{\partial F_h}{\partial u_h} \bigg|_{u_h^H} \right)^T \left[\frac{\partial R_h}{\partial u_h} \bigg|_{u_h^H} \right]^{-1} (f_h - A_h u_h) \tag{3}
$$

By setting

$$
\Psi_h = \left(\frac{\partial F_h}{\partial u_h} \bigg|_{u_h^H} \right)^T \left[\frac{\partial R_h}{\partial u_h} \bigg|_{u_h^H} \right]^{-1}
$$

it follows that Ψ_h must satisfy

$$
\left[\frac{\partial R_h}{\partial u_h} \bigg|_{u_h^H} \right]^T \Psi_h = \left(\frac{\partial F_h}{\partial u_h} \bigg|_{u_h^H} \right)^T \tag{4}
$$

Throughout this paper we will refer to (4) as the adjoint system and to Ψ_h as the adjoint solution. Note that if Ψ_h is known then (3) may be expressed as $F_h(u_h) = F_h(u_h^H) - (\Psi_h)^T (f_h - A_h u_h^H)$ and a value for $F_h(u_h)$ may be found without having calculated u_h explicitly. Of course solving (4) exactly to obtain Ψ_h is likely to be as expensive as obtaining u_h exactly. Hence,

instead of solving the adjoint system on this fine mesh, an approximation to it is solved for on the coarse mesh. This is given by

$$\left[\frac{\partial R_H}{\partial u_H}\right]^T \Psi_H = \left(\frac{\partial F_H}{\partial u_H}\right)^T \qquad (5)$$

This coarse grid adjoint solution is then interpolated onto the fine grid to give $\Psi_h^H = I_h^H \Psi_H$. The correction operation for the functional is given by

$$F_h(u_h) \approx \tilde{F}_h(u_H) = F_h(u_h^H) - (\Psi_h^H)^T R_h(u_h^H) \qquad (6)$$

An estimation of the error in the functional between the two grids has now been obtained simply by solving an additional (adjoint) problem on the coarser grid. Note that we will refer to the expression $(\Psi_h^H)^T R_h(u_h^H)$ in (6) as the "correction" to the functional $F_h(u_h^H)$. A summary of this error estimation procedure is presented in Figure 1.

3.   MODEL PROBLEM

In order to help understand how the above adjoint theory may be applied to a full EHL problem, in this work we focus on a slightly simplified model problem. This is designed to capture the key nonlinear features of the force balance equation and the free boundary for the cavitation position. The elastic deformation is therefore neglected at this stage.

Pressure is solved from a hydrodynamic "Reynolds" equation

$$\frac{d}{dX}\left(H^3 \frac{dP}{dX}\right) - \lambda \frac{dH}{dX} = 0 \qquad (7)$$

with the film thickness given by

$$H(X) = H_0 + \frac{X^2}{2} \qquad (8)$$

1. Solve the system of equations $A_H u_H = f_H$ on the coarser grid
2. Solve the adjoint system (5) on the coarser grid
3. Interpolate u_H and Ψ_H onto the finer grid
4. Calculate the functional $F_h(u_h^H)$ using the interpolated solution
5. Calculate the fine grid residuals $R_h(u_h^H)$ using the interpolated solution
6. Calculate the correction (product of adjoint and residuals)

Figure 1. Summary of the adjoint error estimation procedure

The deformation term is omitted, leaving the separation to be governed only by H_0. The values of H_0 and the cavitation position X_c must be found such that both the force balance equation

$$\int_{X_{-\infty}}^{X_c} P(X)dX = L \tag{9}$$

and the cavitation condition

$$P'(X_c) = 0 \tag{10}$$

are satisfied. In equation (9) $X_{-\infty}$ is defined to be equal to X_c minus a given, constant, domain size (chosen to be sufficiently large as to not influence the solution in the contact region significantly).

3.1   Solution Procedure

For a given value of X_c the Reynolds equation, (7), may be discretized using a second order finite order finite difference scheme, as previously described[10], for example. For simplicity the mesh spacing may be considered to be fixed, at ΔX say, although in practice it will be allowed to adapt in different regions of the domain. In order to satisfy (10) it is necessary to allow X_c to vary until both the discrete forms of (7) and (10) are satisfied together (achieved via an iterative procedure). Other approaches to dealing with the cavitation region may be found elsewhere[11,12,13], however it is important for this work that the cavitation position, X_c, be treated as a continuous variable, and as such the region beyond X_c need not be considered. This allows it to fit more naturally into the theoretical framework introduced above. Finally note that by defining $X_{-\infty}$ to be X_c minus some fixed value, as X_c varies within the solution procedure $X_{-\infty}$ varies too, so that the size of the computational domain remains fixed. This removes the problem of having ΔX depend on X_c (which would make the sparsity pattern of the Jacobian matrix in (5) dense) and also, with the extension to deforming contacts in mind, eliminates the need to recompute the kernel function. The fact that the left-hand boundary moves is countered by the fact that it is chosen to be sufficiently far to the left to make no significant difference to the calculated value of the friction. In summary, the discrete problem that must be solved is to find P_1 to P_{n-1}, H_0 and X_c such that the following residuals are zero:

$$R_i = \Delta X \left(\lambda X_i - \left(\frac{H_{i+\frac{1}{2}}^3 P_{i+1} - (H_{i+\frac{1}{2}}^3 + H_{i-\frac{1}{2}}^3)P_i + H_{i-\frac{1}{2}}^3 P_{i-1}}{(\Delta X)^2} \right) \right) \tag{11}$$

for $i = 1, \ldots, n-1$,

$$R_{H_0} = L - \sum_{i=0}^{n-2} \frac{P_i + P_{i+1}}{2} \Delta X \tag{12}$$

and

$$R_{X_c} = \frac{3P_{n-1} - 4P_{n-2} + P_{n-3}}{2\Delta X} \tag{13}$$

Having fully specified the model problem, attention can be turned to the discrete adjoint formulation.

3.2 Adjoint Problem

As stated in (5) the adjoint system is based upon the transpose of the Jacobian of the residual equations. The Jacobian entries are defined by $\frac{\partial R_i}{\partial P_j}$, $\frac{\partial R_i}{\partial H_0}$, $\frac{\partial R_i}{\partial X_c}$, $\frac{\partial R_{H_0}}{\partial P_i}$, $\frac{\partial R_{H_0}}{\partial H_0}$, $\frac{\partial R_{H_0}}{\partial X_c}$, $\frac{\partial R_{X_c}}{\partial P_i}$, $\frac{\partial R_{X_c}}{\partial H_0}$, $\frac{\partial R_{X_c}}{\partial X_c}$, for $i, j \in 1, \ldots, n-1$. Based on (11) - (13), the sparsity pattern of the Jacobian can be easily obtained and is shown in Figure 2.

The functional that we are interested in for this work is the friction, which for this model problem is given by

$$F(P) = \int_{-\infty}^{X_c} \left(-\frac{\partial P}{\partial X} \frac{H}{2} + \frac{\overline{\eta}}{H} \right) dX \tag{14}$$
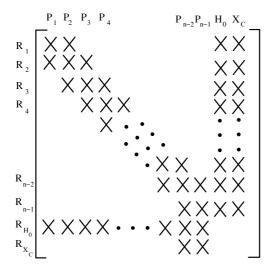
Figure 2. Sparsity pattern for the Jacobian of the residuals

This may be calculated using a simple quadrature scheme, such as the compound midpoint rule, whereby the integrand (by physical analogy we refer to this as the shear stress) is estimated on each cell of the mesh using the pointwise values of P. To form the right-hand side of the adjoint system (5) the derivative of this quadrature expression with respect to each P, along with H_0 and X_c must be obtained: these are easily calculated analytically. Once a solution has been found, the right-hand side of (5) may then be evaluated and Ψ_H may be obtained.

The solution Ψ_H of the adjoint system represents the sensitivity of the friction to each of the residuals. Hence multiplying each of these adjoint variables by the corresponding residual and taking the sum allows an estimate to be obtained of the error in the friction between the two grids. Note that although Ψ_H and u_H are found on the coarser grid the best approximation to the error is obtained by interpolating these to the finer grid before finding the residual $R_h(u_h^H)$ and its product with Ψ_h^H. This is the last expression of equation (6).

4.   RESULTS

In this section a small number of sample results are presented. In all cases, unless stated otherwise, the value of L in (9) is taken as 5.0 and the value of $\bar{\eta}$ in (14) is taken as 20.0.

4.1   Uniform Mesh Results

Before considering a sequence of locally refined meshes, we begin by presenting results on uniform meshes. Table 1 shows the performance of the predicted error in the friction, as calculated using the adjoint approach, by comparing it with the true error when solving on the next mesh. Note that in this context we use the term error to mean $F(u_h^H) - F(u_h)$ (as opposed to $F(u_h^H) - F(u)$ where u is the exact solution of the continuous problem).

The first column of the table shows the grid level for the coarser of the two grids, and has a number of points equal to $2^{g+1} + 1$. Using the solution from this grid, interpolated onto grid $g + 1$, a friction value is calculated which is shown in the second column. Column three shows the correction to this friction, as calculated using the adjoint system solved on the coarse grid g. The corrected friction is shown in column 4, with the "true" friction value for grid $g + 1$ shown in column 5. The measured error between columns 2 and 5 is shown in column 6. The final column shows the ratio of

the measured error to the estimated error (known as the Effectivity Index) and can be seen to approach unity with increasing mesh resolution, which indicates that for uniform grids the friction error estimate is remarkably accurate. If the adjoint solution were not available, it would be necessary to keep computing on finer and finer grids until the friction changed by less than ε, at which point the last (and most expensive) solution does not yield a friction value that is significantly more accurate than the previous. By using this strategy but based upon the adjoint estimate the same accuracy will be achieved but we will have saved the cost of computing a solution on the finest mesh in this sequence.

4.2   Adaptive Mesh Results

Table 2 shows that with non-uniform meshes the adjoint error estimation approach is still reliable, in the sense that the ratio of the predicted correction to the actual difference in friction on consecutive meshes still tends to one as the meshes are refined. Note that in order to obtain these results global mesh refinement, based upon element bisection, has still been used, but now the initial mesh (and hence all subsequent meshes) is non-uniform. Clearly the residual equation (7) has to be modified to reflect this non-uniformity in ΔX and the grid level referred to in the first column of the table indicates the finest level that is present in the mesh.

Having demonstrated that the predicted error is still reliable on non-uniform meshes it is now possible to use these values as the basis for local, rather than global, mesh refinement. It should be noted, however, that the correction value given by the last term in equation (6) is just a single number indicating the current error in the friction and so further information is required in order to determine where the contribution to this error is the greatest. In the following example we base the local refinement on the magnitude of $(\Psi_h^H)_i \times (R_h(u_h^H))_i$ locally, and refer to this as the correction component of mesh point i. Figure 3 shows the computed correction components across the domain after a number of local refinements have been undertaken. Starting from the left it may be seen that the contribution to the estimated friction error gradually increases until the first region of local refinement is reached, whereupon it drops suddenly. The contribution to the error then grows again until the next region of local refinement is reached, and so on. The contribution to the error is always kept below 10^{-7} in this particular example.

Table 1. Adjoint based inter-grid friction error on non-uniform meshes, each with the same refinement

Grid (g)	Interpolated Friction (g)	Calculated Correction	Corrected Friction (g)	Friction (g+1)	Measured Error	Effectivity Index
5	87.95668	15.27956	72.67711	68.02241	19.93427	1.304
6	68.67781	2.64095	66.03686	66.37680	2.30101	0.871
7	66.52919	0.31057	66.21862	66.31442	0.21477	0.691
8	66.35216	0.01504	66.33712	66.34818	0.00398	0.264
9	66.35761	-0.00255	66.36015	66.36125	-0.00365	1.432
10	66.36361	-0.00124	66.36484	66.36496	-0.00135	1.094
11	66.36555	-0.00037	66.36592	66.36593	-0.00038	1.035
12	66.36608	-0.00010	66.36618	66.36618	-0.00010	1.016

Table 2. Adjoint based inter-grid friction error on non-uniform meshes, each with the same refinement

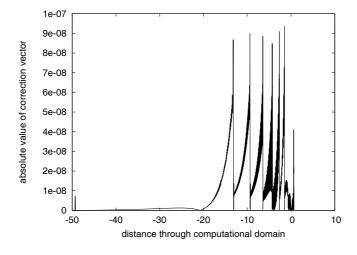| Grid (g)	Interpolated Friction (g)	Calculated Correction	Corrected Friction (g)	Friction (g+1)	Measured Error	Effectivity Index
5	87.66173	-4.56301	92.22474	67.98769	19.67404	-4.311
6	68.65988	2.62800	66.03187	66.36806	2.29181	0.872
7	66.52502	0.30892	66.21611	66.31220	0.21282	0.688
8	66.35111	0.01462	66.33649	66.34762	0.00348	0.238
9	66.35734	-0.00266	66.36000	66.36111	-0.00377	1.417
10	66.36354	-0.00127	66.36481	66.36492	-0.00138	1.093
11	66.36553	-0.00038	66.36591	66.36592	-0.00039	1.035
12	66.36608	-0.00010	66.36618	66.36618	-0.00010	1.016

Figure 3. Plot showing the absolute value of the correction vector, and how it is distributed through local mesh refinement
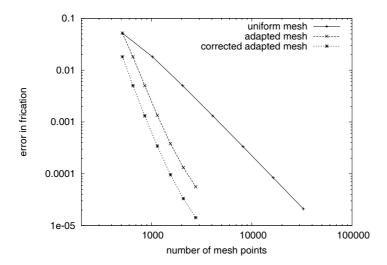
Figure 4. Plot showing error reduction for uniform and adaptive grids

Figure 4 shows the overall effectiveness of this strategy compared to the use of uniform mesh refinement. In this case the plot is of the error in the friction (as compared against a friction value calculated on a so-called "truth mesh" containing approximately 250,000 equally spaced points) versus the total number of nodes present in the mesh. Unsurprisingly the uniform refinement strategy converges most slowly, the next curve shows the error in the friction on the locally refined (adapted) mesh, whilst the final curve shows the error in the corrected friction value on the adapted mesh.

5.   DISCUSSION

Results have been presented which show that the adjoint error estimation approach may be used effectively for a non-linear EHL-like model problem containing a free boundary due to the cavitation condition. The effectivity of this estimate on uniformly refined meshes may be used to provide a reliable stopping criterion without the need to solve on the finest mesh. Furthermore, the components of the correction term are shown to provide an appropriate basis for determining where to refine locally. The resulting meshes can yield solutions of a considerably greater accuracy (in terms of friction, for example) than obtained on correspondingly sized uniform grids.
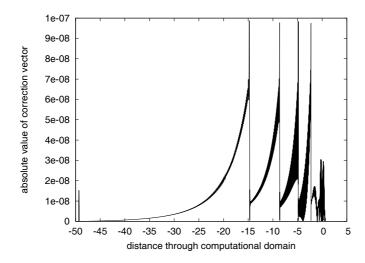
Figure 5. Plot showing the absolute value of the correction vector, and how it is distributed
through local mesh refinement

It should be noted that the adjoint procedure provides an estimate that may be used to control mesh adaptivity based upon a particular quantity of interest. When this quantity is altered (changing the value of $\overline{\eta}$ in (14) for example) then the resulting refinement of the mesh will be altered accordingly. This behaviour is illustrated in Figure 5 which shows the equivalent plot to that of Figure 3 but for the case $\overline{\eta} = 0.0$. Again a sequence of local refinements have been undertaken so as to keep the local contribution to the error below 10^{-7} everywhere but the resulting grid is very different (the regions of change in refinement level can clearly be seen to differ between Figures 3 and 5.

The next stage in this work is to move on to a true EHL line contact problem by introducing elastic deformation and more realistic viscosity and density models. Being highly localised computations, neither of the rheological equations should adversely affect the sparsity of the Jacobian. However, the introduction of the deflection calculation will clearly make the Jacobian dense. One possible solution may be to use the differential deflection method proposed by Evans and Hughes[14] to compute the elastic deformation of the solid. One of the longer term goals of this work is to solve problems with real surface roughness, where it is hoped that adaptation can take place to resolve only those features of most importance to the friction calculation.

References

1 C. E. Goodyer, R. Fairlie, D. E. Hart, M. Berzins, and L. E. Scales, Calculation of Friction in Steady-State and Transient EHL Simulations, in: *Transient Processes in Tribology: Proceedings of the 30th Leeds-Lyon Symposium on Tribology* edited by A. A. Lubrecht and G. Dalmaz (Elsevier, 2004)

2 C. E. Goodyer, R. Fairlie, M. Berzins, and L. E. Scales, Adaptive mesh methods for elastohydrodynamic lubrication, in *ECCOMAS CFD 2001 : Computational Fluid Dynamics Conference Proceedings*, (Institute of Mathematics and its Applications, 2001).

3 S. R. Wu and J. T. Oden, A Note on Application of Adaptive Finite Elements to Elastohydrodynamic Lubrication Problems, *Comm Appl Num Meth*, **3**, 485-494 (1987).

4 A. A. Lubrecht, Numerical solution of the EHL line and point contact problem using multigrid techniques, PhD thesis, (University of Twente, Endschende, The Netherlands, 1987).

5 C. H. Venner, Multilevel Solution of the EHL Line and Point Contact Problems, PhD Thesis, (University of Twente, Endschende, The Netherlands, 1991).

6 C. H. Venner and A. A. Lubrecht, *Multilevel Methods in Lubrication*, (Elsevier, 2000).

7 O. Pironneau, *Optimal Shape Design for Elliptic Systems*, (Springer-Verlag, 1984).

8 N. A. Pierce and, M. B. Giles, Adjoint Recovery of Superconvergent Functionals from PDE Approximations, *SIAM Review* **42**(2), 247-264 (2000).

9 D. A. Venditti and D. L. Darmofal, Grid Adaptation for Functional Outputs: Application to Two-Dimensional Inviscid Flows, *J Comp Phys*, **176**, 40-69 (2002).

10 D. E. Hart, M. Berzins, C. E. Goodyer, P. K. Jimack, and L. E. Scales, Adjoint Error Estimation for EHL-like Models, *Int J Numer Meth Fluids*, **47**, 1069-1075 (2005).

11 S. R. Wu, A Penalty Formulation and Numerical Approximation of the Reynolds-Hertz Problem of Elastohydrodynamic Lubrication, *Int J Eng Sci*, **24**, 1001-1013 (1986).

12 D. Dowson and C. M. Taylor, Cavitation in bearings, *Ann Rev Fluid Mech*, **11**, 35-66 (1979).

13 D. G. Christopherson, A New Mathematical Method for the Solution of Film Lubrication Problems, *Proc Inst Mech Eng*, **146**, 126-135 (1942).

14 H. P. Evans and T. G. Hughes, Evaluation of deflection in semi-infinite bodies by a differential method, *Proc Inst Mech Eng, Part C*, **214**, 563-584 (2000).